



# Battery Charge Controller for 3 Phase Grid Tied PV System

K. Maruthi<sup>1</sup> | M. Venkateswarlu<sup>2</sup>

<sup>1</sup>PG Scholar, Department of EEE, Dr. Samuel George Institute of Engineering, Markapur, Andhra Pradesh, India.

<sup>2</sup>Associate Professor, Department of EEE, Dr. Samuel George Institute of Engineering and Technology, Markapur, Andhra Pradesh, India.

## To Cite this Article

K. Maruthi and M. Venkateswarlu. Battery Charge Controller for 3 Phase Grid Tied PV System. International Journal for Modern Trends in Science and Technology 2022, 8(S02), pp. 85-92. <https://doi.org/10.46501/IJMTST08S0244>

## Article Info

Received: 26 April 2022; Accepted: 24 May 2022; Published: 30 May 2022.

## ABSTRACT

*Due to various causes, including continual price reductions in PV modules, significant development in EVs, and worries about greenhouse gas emissions, the incorporation of solar PV and the EV charging system is highly demanding. As these types of systems become more common in today's era, the improvement of updated technology, like highly efficacious batteries or solar panels, necessitates additional research. Henceforth the PV system is incorporated with Luo converter in this research which enhances the PV system's output voltage gain. The converter utilizes a PI controller along with PWM for improving the overall device performance and monitoring the maximal power point. A three phase VSI is adopted for inverting the input DC voltage along with a three phase induction motor and the resulting harmonics are minimized by LC filter. The simulation is performed by MATLAB and the THD obtained is a minimal value of 2.56 %.*

**Keywords:** PV system, Luo converter, VSI, PI controller, PWM

## 1. INTRODUCTION

Solar energy is currently the most significant energy source, especially for replacing energy derived from fossil fuels like coal, gas and oil. Photovoltaic (PV) cells utilizing solar energy are able to be integrated as roofs of battery-powered vehicles (BEVs) as well as hybrid electric vehicles (HEVs) in the future. Hence, in these vehicles, electric driving ability is significantly increased [1]. It is critical to build and distribute appropriate infrastructure, like EV charging stations, for enabling the deployment of EV in current scenario. On the basis of this pattern, it is clear that ensuring the energy/power supply of EV charging stations is critical. Developing technologies is tedious which continuously provide energy/power, such as PV generation of power as well as the use of systems for energy storage, in order to sustain

growth [2]. Stations for charging of electric vehicle (EV) as well as solar PV panels built are among the growing number of distributed energy resources (DERs) [3]. Significant current spikes are caused by the difference in voltage generated within the capacitor as well as the dc source. Due to the intermittent property of solar PV energy, incorporation of PV systems with energy storage systems as well as other renewable energy sources is performed to ensure reliable operation. A front-end dc-dc boost converter is needed with voltage boosting capability to meet the voltage demand of increased dc-link of ac peak voltage, resulting in widely utilized power conversion of two-stage method [4]. The parallel communication of DC-DC converters with PV panels achieves this ability [5]. To avoid series connection having a large number of PV panels, a DC-DC converter

is needed between the inverter and the PV panel. This converter is also important for ensuring electrical isolation in a PV system's power generation [6].

Several DC-DC converters exist, offering improved gain but generate increased ripples [7]. Boost converters are used as DC-DC converters to increase the PV panel voltage, and their use decreases the ripple current at input obtained from solar panel, improving the panel's reliability and extraction capacity [8]. Boost converters, despite their advantages, have a discontinuous input and output, necessitating the use of more switching machines. This has an effect on the dynamics of the circuit leading to gain fluctuations [9]. To address this disadvantage, a buck-boost converter possessing a large input and output range of voltage and improved performance was developed. It gains an additional input function that expands the dc input voltage range, significantly increasing the PV panel's flexibility while demanding centralized control [10]. In PV systems, a zeta converter is also used to produce low ripple current and higher voltage gain, but the voltage gain is sensitive to inductance leakage [11]. The PV panel's CUK converters had minimal switching losses, better voltage control, and higher reliability, allowing for more flexible operation. Even so, these converters lagged as a result of the sharp speed up/down voltage, affecting precise utilization. Furthermore, since high-power operation necessitates large input and output inductors, and the converter is harmed when connected to a utility grid due to grid voltage fluctuations, CUK converter use is restricted in the medium-low power range [12, 13]. Considering these issues, Luo converter is utilized in this approach for the boosting of input voltage.

Due to the utilization of fast PI controller gains tuning, the dynamic performance is improved, and it also improves an adaptive PI controller, that improves complete device functioning while in solar irradiation changes and variations of grid condition [14]. Since it has the ability of neglecting sudden disruptions as well as maintaining rigidity, the classic PI controller is commonly utilized in a cascaded form for restricting DC-link voltage as well as current in grid. Due to its large stability margin, in PI controller the rules for tuning for grid-connected power converters are often influenced by the symmetrical optimum concept [15]. Due to the intrinsic adaptive abilities, PI controller outperforms the direct duty cycle process. It reduces the difference among

the reference voltage provided by panel voltage and actual voltage [16]. In addition, PWM is exploited since it explicitly produces the duty cycles for the switches with the comparison of modulating signals with carrier waveforms and needs less computing resources and is easier to implement [17]. Utilizing PWM, the converter will monitor the PV maximal power point during stabilization of the resultant voltage to boost system's efficiency of generating power by regulating the duty cycle as well as switching frequency [18]. PV systems are typically integrated into the grid using a voltage source inverter (VSI), which may require a stage to boost if the voltage at dc input is insufficient in all conditions of operations [19]. The VSI is equipped with fundamental frequency pulses, which reduces switching loss and improves conversion performance [20].

Hence in this methodology, an efficient system is designed for electric vehicle which contributes the following.

- Luo converter is utilized for enhancing the input voltage from the PV panel.
- PI controller is exploited which minimizes the difference within the reference voltage provided by panel voltage and actual voltage.
- PWM to monitor the PV maximal power point during stabilization of the voltage at output.
- VSI for converting input dc voltage to ac and LC filter to reduce the current ripples.

## 2. PROPOSED METHODOLOGY

Because of the increased use of battery as well as solar energy, power electronic converters are becoming increasingly important as a link between the source and the load. Systems for harvesting energy like photovoltaic are being studied for maximizing the operational range of electric vehicles. In EV, the supply of PV energy to non-critical systems is carried out inside the power grid on-board. **Figure 1** shows a block representation of the suggested technique.

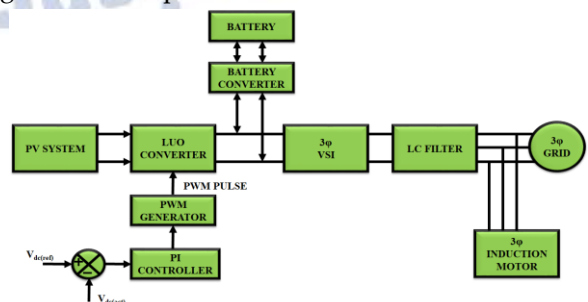


Figure1 Proposed Block Diagram

## A) PHOTOVOLTAIC SYSTEM

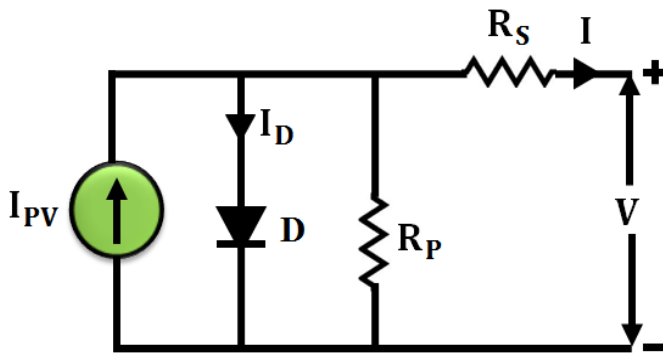


Figure 2 PV system

The circuit diagram of PV system is denoted in Figure 2 and voltage current relation of a PV cell is given as,

$$I = I_{pv} - I_0 \left( \exp \left( \frac{V + R_S I}{\alpha V_t N_s} \right) - 1 \right) - \frac{V + R_S I}{R_p}$$

(1)

Figures 3 and 4 show the single solar panel's IV and PV curves at various irradiances.

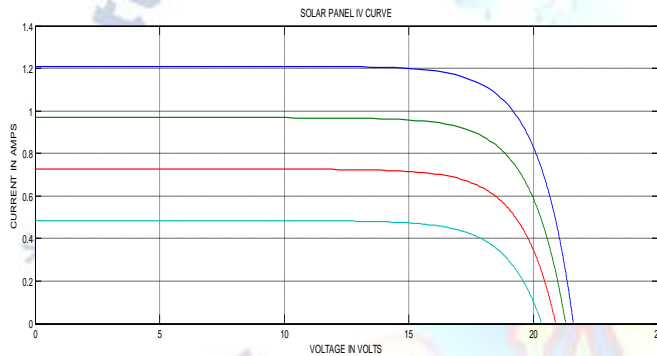


Figure 3 Single solar module IV curve

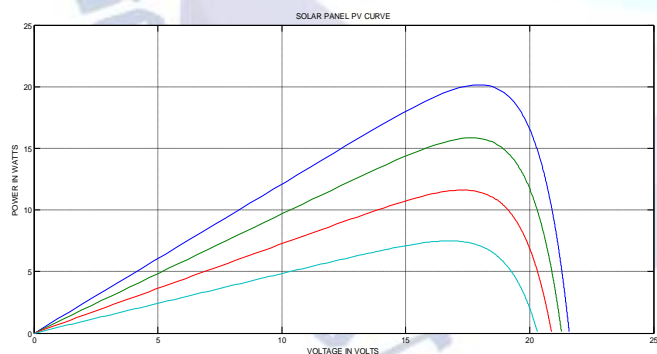


Figure 4 Single solar module PV curve

## B) LUO CONVERTER

The Buck - output Luo converter's connection diagram is given in Figure 5. In the converter circuit, S indicates power switch as well as D indicates the freewheeling diode and inductors are the passive elements for energy storage.

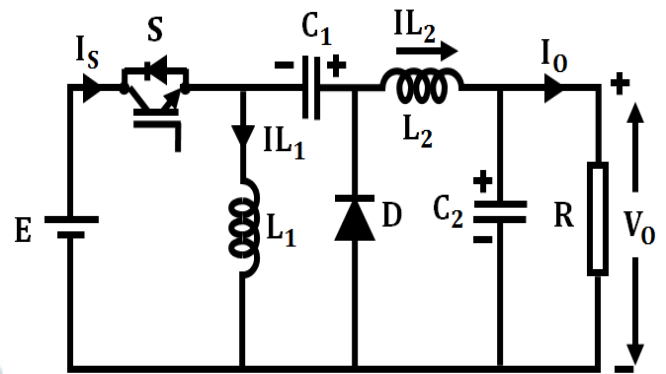


Figure 5 Connection diagram of Luo converter

Inductors L1, L2 as well as capacitors C1, C2 along with load resistance R is present in the circuit. For analyzing the functioning of Luo converter, the operation of circuit is partitioned as two modes as given in Figure 6. At ON condition of switch, the voltage supply E performs charging of the inductor L1. Simultaneously, the source energy is absorbed by the inductor L2 as well as the capacitor C2 supplies the capacitor C1 and the load. In mode 1, in OFF state of the switch, the current drawn from source equals zero. The current  $i_{L1}$  flows across diode for charging the capacitor C1 and current  $i_{L2}$  flows across C2 - R circuit as well as diode D for keeping continuously. The addition of extra filter components like inductor and capacitor is carried out for reducing the harmonic levels of the resultant voltage.

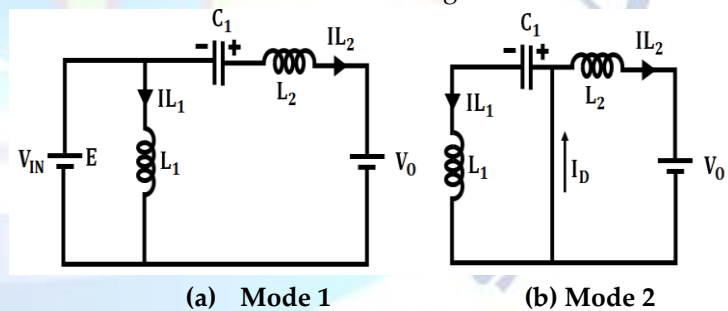


Figure 6 Modes of Operation

The converter's resultant stage comprises of inductor as well as capacitor. Storing and delivering energy towards load as well as smooth the voltage at switch node for producing an output voltage of constant nature. The selection of inductor in direct manner generates impact on the ripple in inductor current and the buck converter current ability. The Inductor shows variation in both material as well as value, and generally possesses 20% tolerance. Inductors possess an inherent DC resistance (DCR) which influences the output stage performance. Reducing the DCR increases the converter's overall performance. It demands an increased load current, and

an inductor with minimal DCR is selected. The DCR is minimal for smaller inductor values, but a trade-off exists within inductance as well as ripple current; when the inductance is lower, the ripple current is higher across the inductor.

## ii) LUO CONVERTER ANALYSIS

Current across inductor  $IL_2$ ,

$$IL_2 = \frac{1-a}{a} IL_1 \quad (2)$$

And duty cycle,

$$a = \frac{T_{on}}{T} \quad (3)$$

Resulting equation for voltage,

$$V_0 = \frac{a}{1-a} V_{in} \quad (3)$$

Across the capacitor  $C_1$ , the average voltage is,

$$V_{c1} = \frac{a}{1-a} V_{in} \quad (4)$$

Peak to peak current across inductor is,

$$\nabla I_{L1} = \frac{aT V_{in}}{L_1} \quad (5)$$

The inductor  $L_1$  value is,

$$L_1 = \frac{aT V_{in}}{\nabla I_{L1}} \quad (6)$$

Peak to peak current across inductor  $L_2$  is,

$$\nabla I_{L2} = \frac{aT V_{in}}{L_2} \quad (7)$$

Equation (7) inductor  $L_2$  value,

$$L_2 = \frac{aT V_{in}}{\nabla I_{L2}} \quad (8)$$

Across series capacitor ( $C_1$ , the charge rises in off period by  $IL_2$  ( $=I_0$ ) as well as reduces in on period by  $IL_1$ . Variations in  $C_1$  charge across the  $C_1$  is zero Peak to peak ripple voltage,

$$\nabla V_{c1} = \frac{1-a}{c_1} T I_1 \quad (9)$$

Equation (9)  $C_1$  value,

$$C_1 = \frac{1-a}{\nabla V_{c1}} T I_2$$

## C) PWM GENERATOR:

The PWM signal is generated by this generator and fed to the Luo converter. It generally chops the reduction of the average power into distinct parts. The voltage as well as average current values are applied to the load side by maintaining the switch ON for more time comparing to OFF time. Because of longer ON duration, the delivered power increases. The major functioning of the PWM generator is generating pulse width modulated gate pulse signal.

## D) PI CONTROLLER

As shown in **Figure 7**, the Proportional Integral (PI) controller is a feedback controller. It controls the plant with a weighted sum of error, as well as the value of integral. PI controllers are applied for controlling the operation and moreover, due to variations in dynamics of

system and operating points. Adaptive PI-controllers forbid manual tuning of time-consumption by offering optimized settings of PI-controller in automatic manner when variation in system dynamics or operating points.

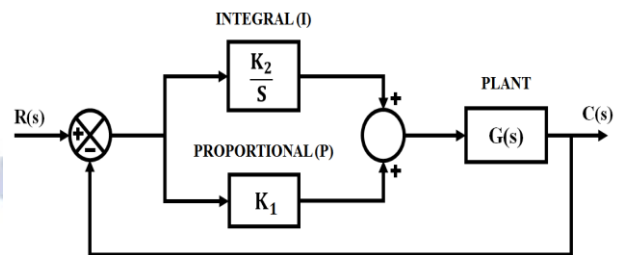


**Figure 7** Basic block of PI Controller

The order and type of system is improved by PI controller. It leads to error in steady state and reduces to zero. PI controller increases damping as well as minimizes maximal overshoot. The bandwidth is decreased and the rise time is increased. The derivative action makes the system steady in the presence of noisy data and this occurs because of derivative action that is sensitive to the increased input frequency terms.

## E) BATTERY

The lithium-ion battery is of rechargeable type and the movement of lithium ions from the negative to the positive electrode while discharging and charging occurs. Even though costly, these batteries possess the merit of low maintenance as well as long duration, absence of memory effect, battery which is rechargeable without complete vacating prior disposal. Here, a Ni-Cd rechargeable battery is utilized which is a device of energy storage that is charged again after being discharged with the application of DC current to its terminals. A rechargeable battery usually replaces one-time use batteries in a more sensible as well as sustainable manner, generating current across a chemical reaction in which consumption of reactive anode occurs.

## F) BATTERY CONVERTER

The bidirectional DC-DC converter which is non-isolated utilized as shown in **Figure 8** works in 2 modes. For bidirectional operation, controlled switches replace diodes. Switch  $S_1$  is triggered for operation in buck mode, and switch  $S_2$  is triggered for operation in boost mode.

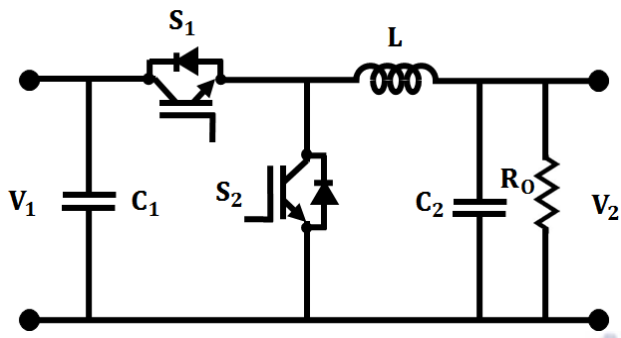


Figure 8 Bidirectional Converter

i) BUCK MODE OPERATION

The Buck mode produces a lower output voltage than the input voltage. For charging the battery, triggering of switch S1 occurs and S2 is maintained off as given in Figure 9. At ON condition of S1, increase in input current occurs and flows across S1 as well as L. At OFF condition of S1, decrease of the inductor current occurs till adjacent cycle.

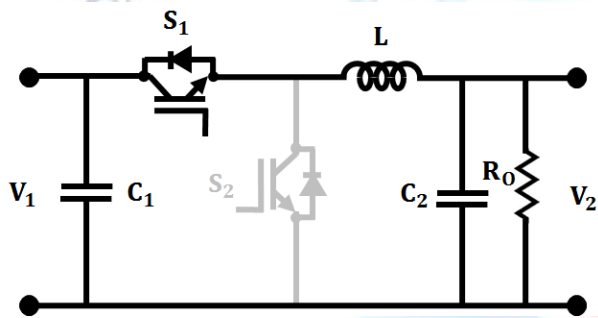


Figure 9 Circuit in Buck mode

ii) BOOST MODE OPERATION

The voltage at output is higher than voltage at input in boost mode. When triggering of switch S2 occurs and at OFF condition of S1, the power is discharged by battery to the load. The functioning of this mode is represented in Figure 10. The current at input increases across inductor L as well as S2 at ON condition of switch S2 and the current at inductor reduces till the adjacent cycle at OFF condition of S2. The stored energy in inductor L flows across the load.

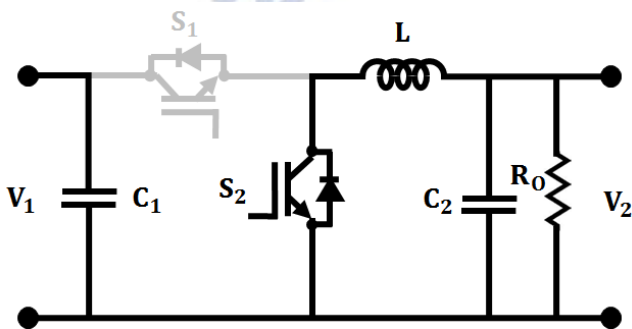


Figure 10 Circuit in Boost Mode

G) 3PHASE VOLTAGE SOURCE INVERTER & LC FILTER

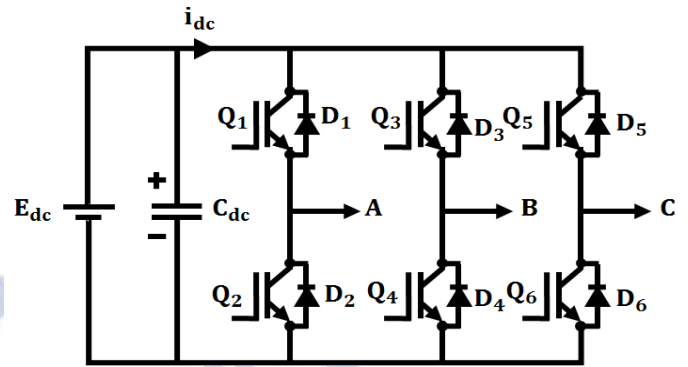


Figure 11 3-phase VSI

Fast and controllable switches are denoted as Q1, Q2, Q3 etc. are while D1, D2, D3 etc. are quick recovery diodes linked with the switches in anti-parallel as given in Figure 11. 'A', 'B' and 'C' are resultant inverter terminals linked to the ac load. Three-phase inverter possesses three terminals of load-phase and the current applied to the inverter switches by the dc bus is regarded as dc link current. The dc link current magnitude frequently varies in step when the switches of inverter are made on, off. A step variation in instant dc link current happens even if a steady power is drawn by the ac load at inverter output. Anyway, the dc link current's average magnitude is positive if average flow of power is from dc bus to ac load.

Depending on the type, the cost, efficiency, losses, size and weight of LC filters are diverse. Moreover, the LC filter consists of minimal inductor and capacitor values. To design the LC filter, it is necessary to determine the maximum ac current ripple. The inductance on the inverter side is specified at rated power along with 5% of the phase current. It is considered that the maximal power factor change of the grid is fixed at 5% when selecting the filter capacitance.

H) 3 PHASE INDUCTION MOTOR

The 3φ AC induction motor is an electric machine that rotates and is developed for operating in a three-phase supply. It is also termed as an asynchronous motor and these motors are divided into two categories: squirrel as well as slip-ring type induction motors. The generation of a rotating magnetic field is required for its operation. These 3φ motors consist of a stator and a rotor that are made up of high magnetic core materials to ease hysteresis loss, eddy current loss and have no electrical connection between them.

The frame of stator is designed utilizing aluminum, cast iron or rolled steel. It offers needed protection and support mechanically for stator laminated windings, core and other ventilation arrangements. The stator is wound with 3 $\phi$  windings that overlap at a 120-degree phase shift and are slotted into laminations. Copper wire and varnish are used to insulate these windings, which are then put into insulated slotted laminations. The rotor of a 3 $\phi$  AC induction motor differs between slip-ring and squirrel-cage induction motors. Two bearings support the shaft of induction motor at every ends ensuring free rotation within the stator and thereby reducing the friction.

### 3. RESULT AND DISCUSSION

The suggested work is implemented in a MATLAB simulation and the results are as follows. Figure 12 shows the solar panel voltage representation of input AC, the source of output voltage is 70(V) attained. Figure 13 represents the Luo converter's input current waveform.

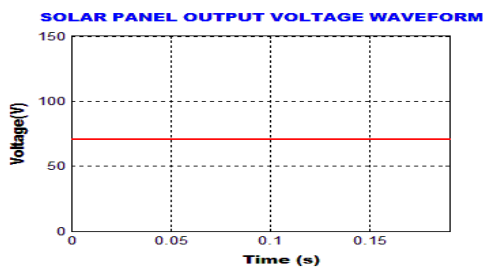


Figure 12 Output voltage waveform of solar panel

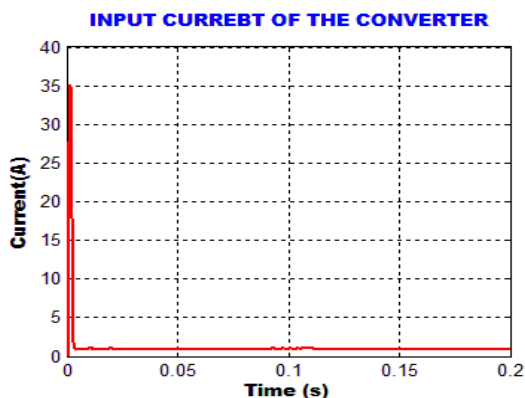


Figure 13 Converter's input current

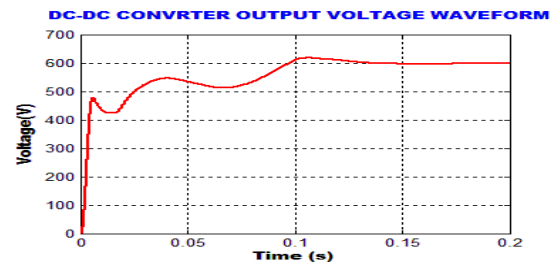


Figure 14 Output voltage waveform of DC-DC converter

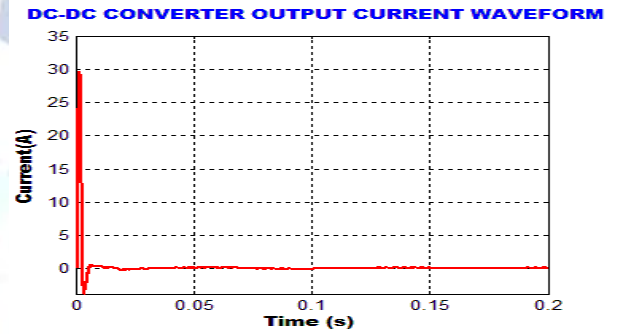


Figure 15 Output current waveform of DC-DC converter

The Luo converter's output voltage and current waveform are given in Figure 14 and 15 respectively.

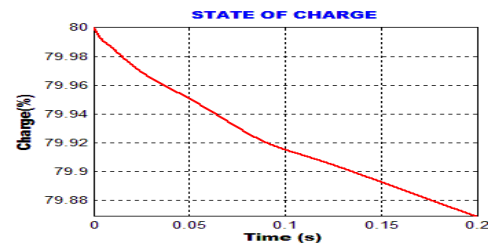


Figure 16 SoC of Battery

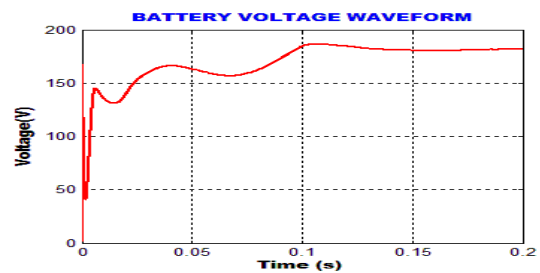


Figure 17(a) Voltage waveform of battery

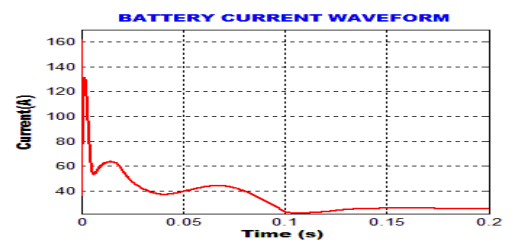
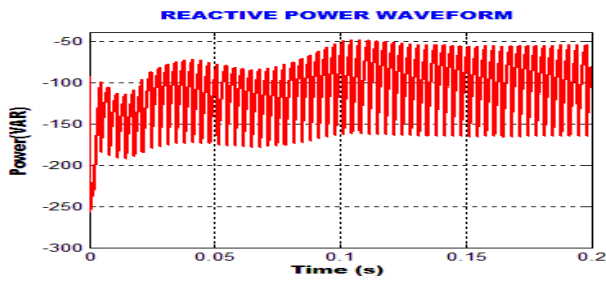
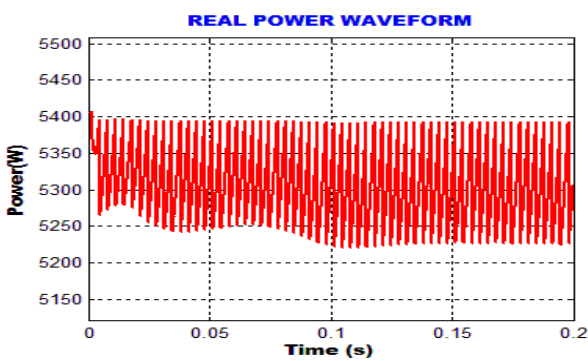


Figure 17(b) Current waveform of battery

The state charge of the output battery voltage and current waveform are given in **Figure 16, 17(a)** and **17(b)** respectively.



**Figure 18** Waveform of reactive power



**Figure 19** Waveform of real power

The **Figure 18** and **19** show the reactive and real power waveforms of the proposed work.

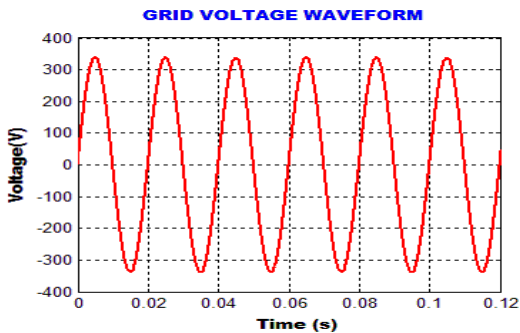


**Figure 20** Waveform of grid voltage

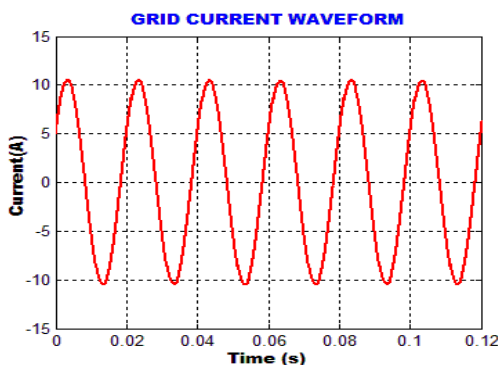


**Figure 21** Waveform of grid current

The output grid voltage and current waveform are given in **Figure 20** and **21** respectively. The grid synchronization with a PI controller accomplishes reactive power correction.

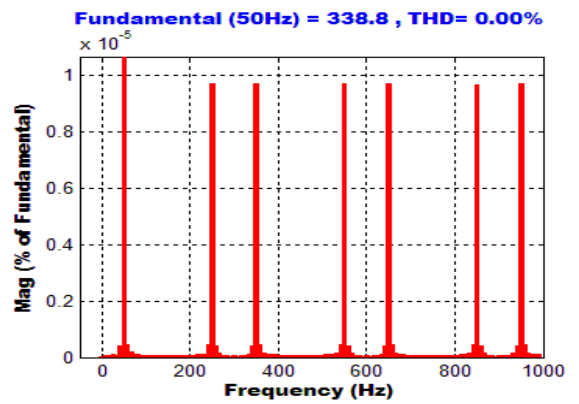


**Figure 22** Voltage waveform THD value

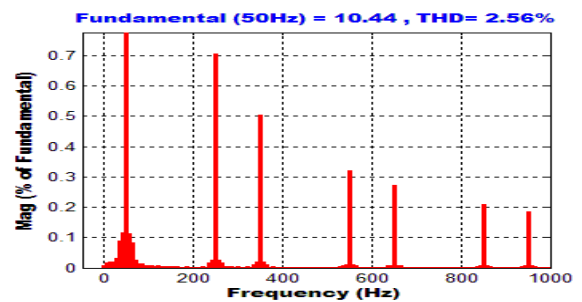


**Figure 23** Current waveform THD value

The input voltage and current THD with a source THD of 2.56 percent is shown in **Figures 22** and **23**.

#### 4. CONCLUSION

In this work, an effective Luo converter with PI controller is projected for a PV system utilizing grid. The output voltage of a PV system is inadequate, so it is supplied to Luo converter which produces the enhanced output. The PI controller is exploited which minimizes the difference within the reference voltage provided by panel voltage and actual voltage. The converter functions regardless of irradiance fluctuations, resulting in higher voltage gain and minimal switching losses. For converting fixed DC voltage to variable frequency AC voltage, a 3 $\phi$  VSI is used. The VSI is used for converting input dc voltage to ac and LC filter to reduce current ripples. The introduced approach is validated by MATLAB simulation and efficient results are obtained with a THD value of 2.56 %. Also, the obtained finding

confirms the controller's capacity to regulate the power flow balance during various transients caused by changes in solar irradiation, change in the storage battery's charging/discharging current and connection/disconnection of EV. As a result, the proposed system offers increased power quality, grid synchronization and reduced distortion.

### Conflict of interest statement

Authors declare that they do not have any conflict of interest.

### REFERENCES

- [1] Christian Schuss;TapioFabritius;BerndEichberger;TimoRahkonen, 2019, "Impacts on the Output Power of Photovoltaics on Top of Electric and Hybrid Electric Vehicles", IEEE Transactions on Instrumentation and Measurement, Vol: 69, No: 5, pp: 2449 – 2458.
- [2] MyungJaeShin;Dae-HyunChoi;Joongheon Kim, 2019, "Cooperative Management for PV/ESS-Enabled Electric Vehicle Charging Stations: A Multiagent Deep Reinforcement Learning Approach", IEEE Transactions on Industrial Informatics, Vol: 16, No: 5, pp: 3493 – 3503.
- [3] Zhaoxiliu;QiuweiWu;MohammadShahidehpour;CanbingLi;ShaojunHuang;Wei Wei, 2018, "Transactive Real-Time Electric Vehicle Charging Management for Commercial Buildings With PV On-Site Generation", IEEE Transactions on Smart Grid, Vol: 10, No: 5, pp: 4939 – 4950.
- [4] Sze Sing Lee;Yam P. Siwakoti;Chee Shen Lim;Kyo-Beum Lee, 2020, "An Improved PWM Technique to Achieve Continuous Input Current in Common-Ground Transformerless Boost Inverter", IEEE Transactions on Circuits and Systems II: Express Briefs, Vol: 67, No: 12, pp: 3133 – 3136.
- [5] I. Anand;SubramaniamSenthilkumar;DipankarBiswas;M. Kaliamoorthy, 2018, "Dynamic Power Management System Employing a Single-Stage Power Converter for Standalone Solar PV Applications", IEEE Transactions on Power Electronics, Vol: 33, No: 12, pp: 10352 – 10362.
- [6] RuiLi;Fangyuan Shi, 2019, "Control and Optimization of Residential Photovoltaic Power Generation System With High Efficiency Isolated Bidirectional DC–DC Converter", IEEE Access, Vol: 7, pp: 116107 – 116122.
- [7] SaptarshiDe;O. V. Gnana Swathika;NilanjanTewari;Anantha Krishnan Venkatesan;UmashankarSubramaniam;Mahajan Sagar Bhaskar;SanjeevikumarPadmanaban;ZbigniewLeonowicz;Massimo Mitolo, 2020, "Implementation of Designed PV Integrated Controlled Converter System", IEEE Access, Vol: 8, pp: 100905 – 100915.
- [8] Md Waseem Ahmad;Naga Brahmendra Yadav Gorla;HasmatMalik;Sanjib Kumar Panda,2021, "A Fault Diagnosis and Postfault Reconfiguration Scheme for Interleaved Boost Converter in PV-Based System", IEEE Transactions on Power Electronics, Vol: 36, No: 4, pp: 3769 – 3780.
- [9] Balaji Chandrasekar ;ChellammalNallaperumal; Sanjeevikumar Padmanaban;Mahajan Sagar Bhaskar;Jens Bo Holm-Nielsen; ZbigniewLeonowicz;Samson O. Masebinu,2020, "Non-Isolated High-Gain Triple Port DC–DC Buck-Boost Converter With Positive Output Voltage for Photovoltaic Applications", IEEE Access, Vol: 8, pp: 196500 – 196514.
- [10] Qingyun Huang;Alex Q. Huang;RuiyangYu;engkunLiu;Wensong Yu, 2019, "High-Efficiency and High-Density Single-Phase Dual-Mode Cascaded Buck–Boost Multilevel Transformerless PV Inverter With GaN AC Switches",IEEE Transactions on Power Electronics, Vol: 34, No: 8, pp: 7474 – 7488.
- [11] António Manuel Santos Spencer Andrade; LucianoSchuch; MarioLúcio da Silva Martins, 2017, "High Step-Up PV Module Integrated Converter for PV Energy Harvest in FREEDM Systems", IEEE Transactions on Industry Applications, Vol: 53, No: 2, pp: 1138 – 1148.
- [12] Sanjeevikumar Padmanaban;NeerajPriyadarshi;Mahajan Sagar Bhaskar;Jens Bo Holm-Nielsen;EklasHossain;Farooque Azam, 2019, "A Hybrid Photovoltaic-Fuel Cell for Grid Integration With Jaya-Based Maximum Power Point Tracking: Experimental Performance Evaluation",IEEE Access, Vol: 7, pp: 82978 – 82990.
- [13] Byeongcheol Han;Jih-ShengLai;Minsung Kim, 2018, "Dynamic Modeling and Controller Design of Dual-Mode Cuk Inverter in Grid-Connected PV/TE Applications",IEEE Transactions on Power Electronics, Vol: 33, No: 10, pp: 8887 – 8904.
- [14] Nishant Kumar;IkhlqHussain;BhimSingh;Bijaya Ketan Panigrahi, 2018, "Implementation of Multilayer Fifth-Order Generalized Integrator-Based Adaptive Control for Grid-Tied Solar PV Energy Conversion System", IEEE Transactions on Industrial Informatics, Vol: 14, No: 7, pp: 2857 – 2868.
- [15] Rachid Errouissi;AhmedAl-Durra;S. M. Muyeen, "Design and Implementation of a Nonlinear PI Predictive Controller for a Grid-Tied Photovoltaic Inverter", IEEE Transactions on Industrial Electronics, Vol: 64, No: 2, pp: 1241 – 1250.
- [16] Muralidhar Killi;SusovonSamanta, 2018, "Voltage-Sensor-Based MPPT for Stand-Alone PV Systems Through Voltage Reference Control", IEEE Journal of Emerging and Selected Topics in Power Electronics, Vol: 7, No: 2, pp: 1399 – 1407.
- [17] JiangfengWang;HongfeiWu;TianyuYang;LiZhang;Yan Xing, 2018, "Bidirectional Three-Phase DC–AC Converter With Embedded DC–DC Converter and Carrier-Based PWM Strategy for Wide Voltage Range Applications", IEEE Transactions on Industrial Electronics, Vol: 66, No: 6, pp: 4144 – 4155.
- [18] ZheShi;YingjunGuo;PengchengLi;Hexu Sun, 2020, "A Boost CLLC Converter Controlled by PWM and PFM Hybrid Modulation for Photovoltaic Power Generation", IEEE Access, Vol: 8, pp: 112015 – 112026.
- [19] M. S. Hassan;Ahmed Abdelhakim; MasahitoShoyama; JunImaoka;Gamal M. Dousoky, 2020, "Three-Phase Split-Source Inverter-Fed PV Systems: Analysis and Mitigation of Common-Mode Voltage", IEEE Transactions on Power Electronics, Vol: 35, No: 9, pp: 9824 – 9838.
- [20] Rajan Kumar;Bhim Singh, 2019, "Grid Interactive Solar PV-Based Water Pumping Using BLDC Motor Drive", IEEE Transactions on Industry Applications, Vol: 55, No: 5, pp: 5153 – 5165.